Phys. Status Solidi A **214**, No. 6, 1600932 (2017) / **DOI** 10.1002/pssa.201600932

physica status solidi a
www.pss-a.com
applications and materials science

Dependence of dark current and photoresponse on polarization charges for AlGaN-based heterojunction p–i–n photodetectors

Hai-feng Chen[1,2], Yi-Ren Chen[*,1], Hang Song[,1], Zhi-Ming Li[1], Hong Jiang[1], Da-Bing Li[1], Guo-Qing Miao[1], Xiao-Juan Sun[1], and Zhi-Wei Zhang[1]**

[1] State Key Laboratory of Luminescence and Applications, Changchun Institute of Optics, Fine Mechanics, and Physics, Chinese Academy of Sciences, 3888 Dong Nanhu Road, Changchun 130033, People's Republic of China
[2] University of Chinese Academy of Sciences, Beijing 100039, People's Republic of China

Received 9 December 2016, revised 13 February 2017, accepted 14 February 2017
Published online 7 March 2017

Keywords AlGaN, heterojunction, photodetectors, polarization

[*] Corresponding author: e-mail chenyr@ciomp.ac.cn, Phone/Fax: +86 431-84627073
[**] e-mail songh@ciomp.ac.cn, Phone/Fax: +86 431-84627073

The influence of the polarization charges on the properties of AlGaN-based heterojunction p–i–n ultraviolet photodetectors was investigated. It is found that the polarization charges at the hetero-interface can enhance the electric field intensity and result in an increased dark current. On the contrary, the polarization charges can lower the photoresponse because the direction of polarization electric field is opposite to the applied electric field in the light absorption layer.

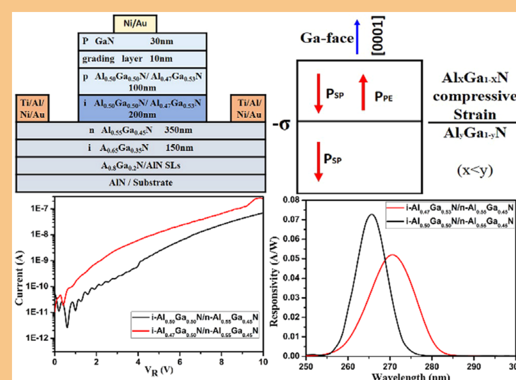

© 2017 WILEY-VCH Verlag GmbH & Co. KGaA, Weinheim

1 Introduction The solid-state solar-blind ($\lambda < 290$ nm) ultraviolet (UV) photodetectors (PDs) based on AlGaN ternary alloy material have drawn a great deal of attention in the defence, commercial, and scientific arenas, such as non line-of-sight confidential communications, the detection of corona discharges in high voltage transmission lines and equipment, flame detection and monitoring, UV environmental monitoring, and UV astronomy [1–3]. The AlGaN material system is advantageous for making solar-blind devices, because $Al_xGa_{1-x}N$, in its wurtzite structure, has a tunable band gap. This can be done by regulating the composition of Al from $x = 0$ (3.4 eV) to 1 (6.2 eV), covering the whole range of solar-blind wavelengths, and using intrinsic solar-blind instead of complex and costly filters [4]. The heterojunction p–i–n structure attracts particular interest due to its intrinsic advantages: the cut-off wavelengths can be modified by changing the Al mole fractions in the AlGaN window layer and absorbing layer, the diffusion limited carrier transport in photodiodes is eliminated, and a direct control of the quantum efficiency through changing the thickness of the intrinsic layer [5]. So far, high performance AlGaN-based heterojunction p–i–n PDs have been reported [6–10]. However, it should be noted that some issues are also introduced during epitaxial growth, such as numerous trapping levels which

© 2017 WILEY-VCH Verlag GmbH & Co. KGaA, Weinheim

existed in the forbidden band because of the lattice mismatch between the different AlGaN films, and these levels may capture and emit free carriers to the conduction or valence bands because of thermal exchange processes or tunneling [11]. In addition, the fixed interface polarization charges are also introduced at nitride hetero-interfaces due to the piezoelectric and spontaneous polarization, which leads to potential barriers, band bending, and internal electric field [12–14]. The polarization effects of wurtzite III-nitrides have been reported to play an important role in the design of hetero-junctions electronic devices [15–17]. However, how the polarization-induced charges play a role in electrical and optical properties of AlGaN-based p–i–n PDs is unknown. There are only a few studies which refer to the polarization charges in AlGaN-based APDs [18–20]. A more detailed characterization and a more complete understanding of the polarization charges on the performance of AlGaN-based p–i–n PDs are desirable to further optimize the design of the devices. Thus, in this work, the influence of the fixed interface polarization charges on the performance of AlGaN-based p–i–n PDs is investigated.

2 Experimental To simplify analysis of the polarization charges and separate the effects of polarization charges from other factors that influence device characteristics, a couple of similar AlGaN-based heterojunction p–i–n PDs were designed. The schematic cross section of device is depicted in Fig. 1. The difference of Al mole fraction between the i-AlGaN absorbing layer and the n-AlGaN contact layer is designed for generating polarization charges, and the small difference of Al composition between the i-AlGaN layers of the two samples is designed to obtain a slight discrepancy of polarization charges.

The AlGaN-based heterojunction p–i–n structures were grown by low-pressure metalorganic chemical vapor deposition (MOCVD) on 2-in. diameter c-plane (0001) sapphire substrates. In the experiment, trimethylaluminium (TMAl), trimethylgallium (TMGa) and ammonia (NH_3) were used as sources of Al, Ga, and N, respectively. The n-type and p-type dopants were doped with silane (SiH_4) and biscyclopentadienyl magnesium (Cp_2Mg), respectively. Deposition was initiated with the AlN buffer layer grown by the normal two-step method [21], followed by a 10 period AlN/$Al_{0.8}Ga_{0.2}N$ superlattices topped with a 150-nm-thick undoped $Al_{0.65}Ga_{0.35}N$ layer. Next, it is followed by the p–i–n structure, consisting of a 350-nm-thick n-$Al_{0.55}Ga_{0.45}N$ window layer, a 200-nm lower Al component $Al_{0.50}Ga_{0.50}N$/$Al_{0.47}Ga_{0.53}N$ unintentionally doped absorbing layer and a 150-nm p-$Al_{0.50}Ga_{0.50}N$/$Al_{0.47}Ga_{0.53}N$ layer. Then, finished with a 10 nm Al component grading p-type AlGaN layer followed by a 30-nm p-GaN contact layer. Last, an in situ anneal was performed to activate the magnesium p-dopant. Sample A has an i-$Al_{0.50}Ga_{0.50}N$ absorption layer while sample B has an i-$Al_{0.47}Ga_{0.53}N$ absorption layer. The electron concentration in Si-doped n-$Al_{0.55}Ga_{0.45}N$ layers is 1×10^{18} cm^{-3}. The hole concentration in Mg-doped p-AlGaN and p-GaN layers is 2×10^{17} and 1×10^{18} cm^3, respectively.

The device fabrication process is as follows: firstly, the circular-mesa devices were defined using a conventional photolithography process followed by an inductively coupled plasma (ICP) etching step, which was etched down to the n-$Al_{0.55}Ga_{0.45}N$ ohmic contact layer and formed a 500-μm-diameter mesa. Secondly, the samples were treated by a photo-electrochemical method to recover the damage made by ICP etching to reduce the leakage current [22]. Thirdly, the n-type ohmic contact was finished by depositing Ti/Al/Ni/Au (30/100/150/200 nm) metal layers by using electron-beam evaporation system followed by annealing in N_2 ambient. Last, the p-type GaN ohmic contact was formed by depositing Ni/Au (20/200 nm) metal layers followed by annealing in N_2 ambient.

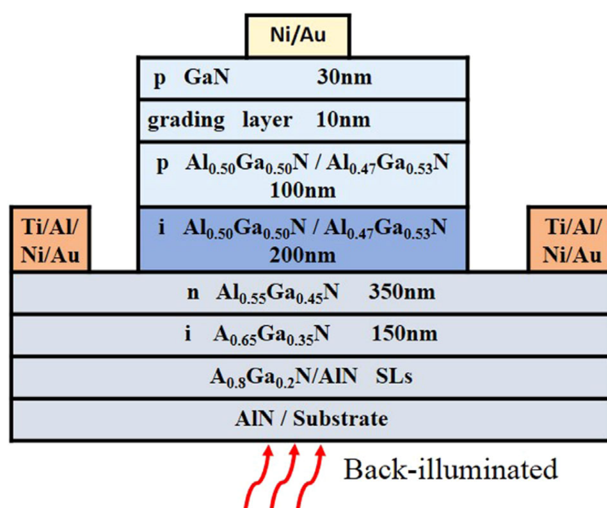

Figure 1 Schematic structure of the AlGaN heterojunction p–i–n photodiodes.

3 Results and discussion The current-voltage (*I–V*) characteristics of the devices at room temperature were carried out by using a Keithley 237 source meter under dark conditions and the curves of the fabricated PDs under different reverse biases are shown in Fig. 2.

As shown in Fig. 2, the dark current of both samples A and B exhibits exponential dependence on the bias voltage with two different exponents, which implies that the current transport is dominated by two kind of tunneling mechanisms when increasing the reverse bias [23]. In addition, from Fig. 2(a), it is found that the measured dark current of sample A is smaller than that of sample B. To further understand the difference of dark current between samples A and B, several factors need to be taken into consideration. Firstly, we measure the full width at half maximum (FWHM) of the X-ray rocking curve (XRC) for both of the samples, as shown in Fig. 3. It is known that high dislocations can contribute to an increase in the dark current [24].

The measured XRC-FWHM shows a small difference between samples A and B. Therefore, the difference of dark

© 2017 WILEY-VCH Verlag GmbH & Co. KGaA, Weinheim

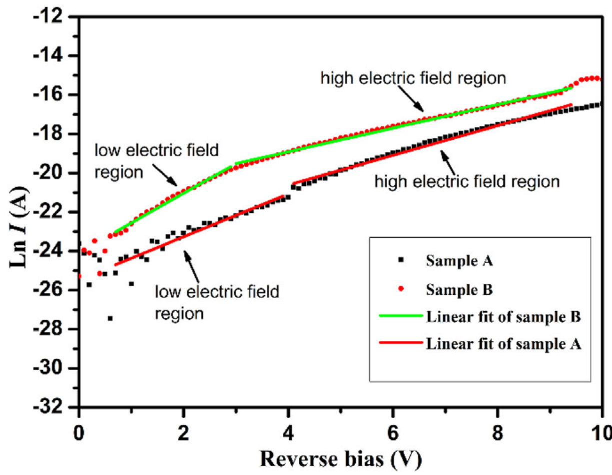

Figure 2 Reverse current-voltage characteristics of AlGaN heterojunction p–i–n PDs in a semi-ln plot.

current may not be dominated by the difference in dislocation density. Secondly, the dark current of many A and B samples are also investigated. The variation of the dark current shows almost the same trend, which means the fabrication-related issue is not the dominating factor. Thirdly, due to the existence of the conduction band offsets at the hetero-interface as shown in Fig. 4, and the conduction band offsets are calculated to be 0.097 and 0.154 eV for $Al_{0.5}Ga_{0.5}N/Al_{0.55}Ga_{0.45}N$ and $Al_{0.47}Ga_{0.53}N/Al_{0.55}Ga_{0.45}N$ respectively [25], the band offsets create a barrier which may impede the injection of electrons from the i-AlGN layer to the n-AlGN layer. Thus, it is expected that the dark current of sample B with high barrier would be lower than that of sample A, however, our results show the opposite. Based on the analysis mentioned above, we think that the hetero-interface may dominate the difference of the dark current between samples A and B.

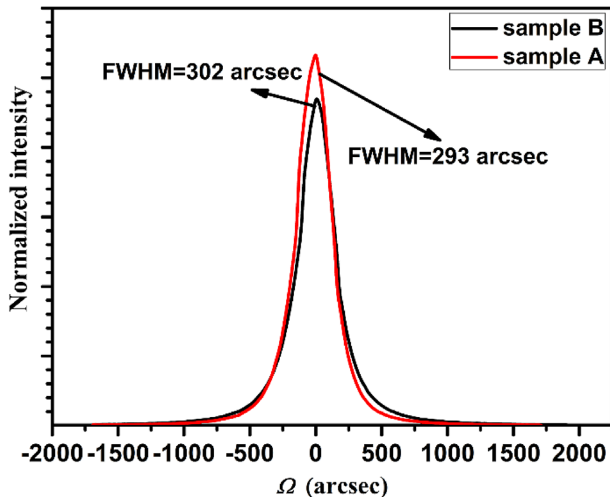

Figure 3 The (0002) XRC of the i-AlGN epilayers in AlGaN-based p–i–n PDs structure.

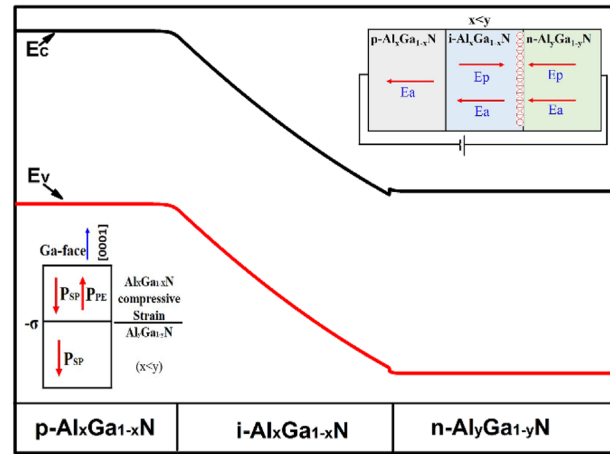

Figure 4 Illustration of band alignment of AlGaN-based p–i–n photodiode. Inset (bottom left corner) shows the direction of the spontaneous P_{SP} and piezoelectric polarization P_{PE} in AlGaN heterostructure. Inset (top left corner) shows the direction of applied electric field E_a and polarization electric field E_p in AlGaN p–i–n structure.

As shown in the inset at the bottom left corner of Fig. 4, a lower Al composition in i-AlGaN layer is employed for the hetero-structure, and the fixed negative polarization charges are introduced at the interface of i-$Al_xGa_{1-x}N$/n-$Al_yGa_{1-y}N$ ($x < y$) because of spontaneous and piezoelectric polarization. The fixed polarization charge density could be calculated with the Al-composition-dependent model proposed by Ambacher et al [25]. The fixed polarization charge density σ is defined by

$$\sigma(P_{SP} + P_{PE}) = P(Al_yGa_{1-y}N) - P(Al_xGa_{1-x}N) \quad (1)$$

where P is the sum of the piezoelectric and spontaneous polarization and is determined by

$$P = P_{PE} + P_{SP}$$

the piezoelectric polarization P_{PE} in the direction of the c-axis can be determined by

$$P_{PE} = 2\frac{a - a_0}{a_0}\left(e_{31} - e_{33}\frac{C_{13}}{C_{33}}\right) \quad (2)$$

where e_{33}, e_{31} are the piezoelectric coefficients, and a is the lattice constants of the strained layer, C_{13} and C_{33} are elastic constants. And the spontaneous polarization can be determined by

$$P_{SP}(x) = (-0.052x - 0.029) \quad (3)$$

Thus, the amount of the polarization induced sheet charge density, σ/e, bound at the interfaces i-$Al_{0.50}Ga_{0.50}N$/n-$Al_{0.55}Ga_{0.45}N$ and i-$Al_{0.47}Ga_{0.53}N$/n-$Al_{0.55}Ga_{0.45}N$ are calculated to be 2.9×10^{12} and $3.5 \times 10^{12}\,cm^{-2}$, respectively. All the parameters in Eqs. (1)–(3) can be found in

© 2017 WILEY-VCH Verlag GmbH & Co. KGaA, Weinheim

Ref. [25]. In order to compensate for the negative polarization induced charges, the donors in n-$Al_{0.55}Ga_{0.45}N$ layer will be further ionized and cause a depletion region in the n-$Al_{0.55}Ga_{0.45}N$ layer. This leads to an increase electric field in the n-$Al_{0.55}Ga_{0.45}N$ side and a voltage drop in the layer, and also increases the conduction band bending of the n-$Al_{0.55}Ga_{0.45}N$ layer at the hetero-interface. When applying an external bias voltage, the electric field at n-$Al_{0.55}Ga_{0.45}N$ side can be enhanced because the polarization induced electric field in the n-$Al_{0.55}Ga_{0.45}N$ layer has the same direction as the reverse bias electric field, as shown in the inset at the top right corner of Fig. 4.

In order to understand the effect of the polarization field on the carrier transport of photodetectors, we calculated the polarization electric field of the i-AlGaN/n-AlGaN hetero-interface, as shown in Fig. 5(b). The calculated results show that the polarization field increases with the polarization charge. And the reverse current transport processes can be explained as Fig 5(a) illustrates. At low negative bias region,

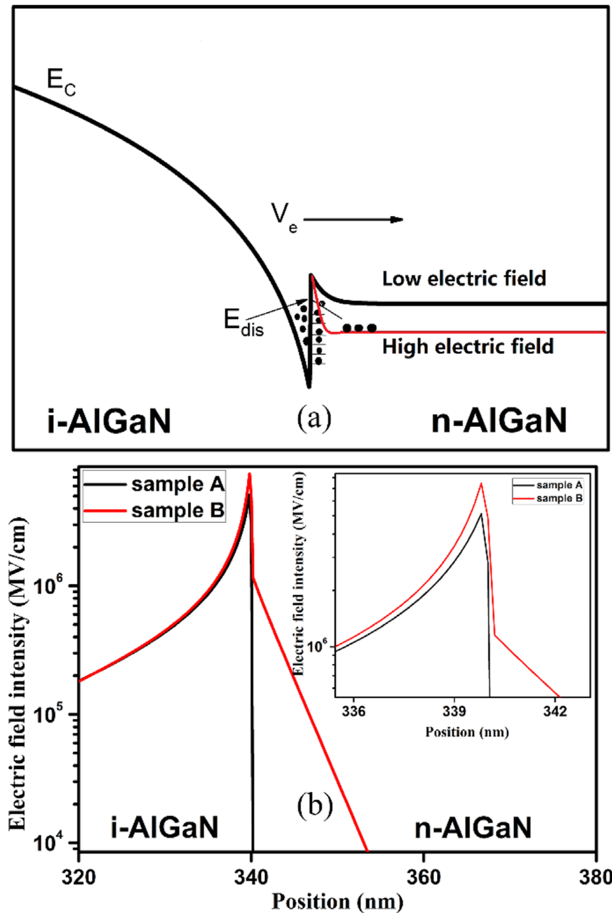

Figure 5 (a) Schematic diagram of the reverse current transport mechanism in hetero-junction AlGaN-based p–i–n PDs. The solid dots represent electrons accumulated at the hetero-junction. (b) polarization electric field intensity of i-AlGaN/n-AlGaN hetero-interface.

the conduction band bending of the n-$Al_{0.55}Ga_{0.45}N$ layer at the hetero-interface is slight. Meanwhile, the dark current exhibits exponential dependence on the bias voltage. The transport processes can be described by the emission of electrons from a shallow trapped state near the i-AlGaN/n-AlGaN hetero-interface into a continuum of states which is associated with each conductive dislocation and tunneling via dislocation. This is based on the Frenkel–Poole emission mode [26]. It is also found to be the sources of reverse bias gate leakage current of AlGaN/GaN HEMTs [27]. The current density associated with Frenkel–Poole emission is given by

$$J \propto C\mathrm{E}\exp\left[-\frac{q\left(\varphi_{\mathrm{B}}-\sqrt{\frac{q\mathrm{E}}{\pi\varepsilon}}\right)}{k_{\mathrm{B}}T}\right] \tag{4}$$

where C is the constant, E is the applied electric field, q is the elementary charge, φ_{B} is the potential barrier for the trap energy state for an electron in zero applied electric field, k_{B} is the Boltzmann's constant, T is the absolute temperature and ε is the permittivity. Furthermore, the FP emission is expressed as

$$\ln\left({}^{J}/_{E}\right) = m(T)\sqrt{E} + C(T)$$

$$m(T) = \frac{q}{k_{\mathrm{B}}T}\sqrt{\frac{q}{\pi\varepsilon}}$$

$$C(T) = \ln C - \frac{q\varphi_B}{k_{\mathrm{B}}T}$$

It can be seen that the FP emission current is dependent on both the energy depth of the trap states and the intensity of electric field.

For high electric field region, the conduction band bends strongly. A large number of electrons can tunnel through the barrier directly. And the electron tunneling probability follows the equation:

$$P = \exp\left\{-\frac{4\pi}{h}(2m)^{\frac{1}{2}}\int_a^b [V(x)-V]^{\frac{1}{2}}dx\right\} \tag{5}$$

where $V(x)$, V, and m are the one-dimensional potential barrier, the electron energy and the particle mass, respectively. For a triangular barrier, the electron tunneling probability is described by

$$P = \exp\left[-\frac{8\pi}{3h}(2m)^{\frac{1}{2}}(E_{\mathrm{g}})^{\frac{3}{2}}\left(\frac{1}{qE}\right)\right] \tag{6}$$

where E_{g} is band gap. Due to tunneling current $I \propto$ tunneling probability P, it means tunneling current is strongly

© 2017 WILEY-VCH Verlag GmbH & Co. KGaA, Weinheim

dependent on the intensity of electric field. Therefore, both the trap energy level of electron emission and electron direct tunneling contribute to the dark current of the high electric field region.

Based on the analysis above, the polarization charge is thought to contribute to the difference in dark current between samples A and B and to significantly affect the *I–V* characteristics of the hetero-junction AlGaN-based p–i–n PDs.

To further understand the polarization charges at the hereto-interface, the spectral responsivity measurements of heterojunction p–i–n photodiodes is carried out, as shown in Fig. 6. The spectral responsivity is measured using a xenon lamp as a light source, a chopper, a monochromator, a lock-in amplifier, a Keithley 6487 dc source, and a calibrated UV-enhanced silicon photodetector. Fig. 6 exhibits a zero bias peak responsivity of 0.072 A/W at 265 nm for sample A and a 0.060 A/W at 270 nm for sample B. And there is a sharp decay of photoresponse near 255 nm for both samples A and B, corresponding to the short-wavelength cut-off of n-$Al_{0.55}Ga_{0.45}N$ layer. The difference in long-wavelength cut-off results from the i-$Al_xGa_{1-x}N$ absorption layer with lower Al mole fraction. The inset of Fig. 6 shows a detailed comparison of peak responsivity for the PDs working in different reverse bias. It is found that sample A exhibits a greater photo-responsivity at reverse bias range from 0 to −5 V.

To analyze the differences of responsivity between samples A and B, it is necessary to consider the light absorption efficiency and the carrier collection efficiency. However, due to the large absorption coefficient of the direct-bandgap AlGaN material system [28], the influence of small differences of Al mole fraction on the absorption coefficient in i-$Al_xGa_{1-x}N$ layer can be neglected. Thus, the carrier collection efficiency is the key limiting factor. It is known that high dislocation density exists in AlGaN layer due to heteroepitaxy [29], which can lead to

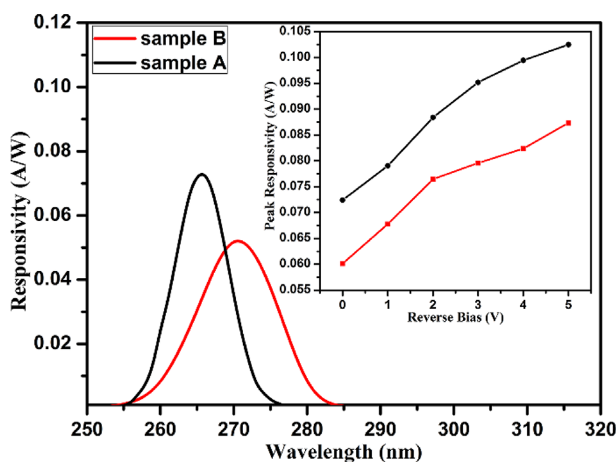

Figure 6 Spectral response characteristics of samples A and B measured under the zero bias. The inset shows the peak responsivity as a function of reverse bias voltage in samples A and B.

significant recombination loss of photo-generated carriers. A way to minimize recombination loss is to reduce the carrier transit time by applying a higher electrical field within the depletion region. But, the direction of the polarization electric field in i-$Al_xGa_{1-x}N$ absorption layer induced by these negative charges is opposite to the applied electric field, as shown in the inset at top left corner of Fig. 4. The effective electric field is weakened. In addition, the fixed negative polarization charges also can attract a number of holes to accumulate at the interface. Therefore, The collection efficiency of the photogenerated holes is reduced.

From the performance of photoresponsivity between samples A and B, it indicates that an increase of negative polarization charge would lower the photoresponse.

4 Conclusions We have experimentally investigated the effect of polarization charges at the hetero-interface on the dark current and photoresponsivity characteristics of AlGaN-based heterojunction p–i–n PDs. The experimental results is in a qualitative agreement with the numerical data produced by Wang et al. [20], which had simulated the effects of polarization charge density on the dark current and photoresponse characteristics in detail. Increasing the fixed negative polarization charges have a significant impact on the performance of the heterostructure AlGaN-based p–i–n PDs. Hence, optimizing the device design to reduce the polarization charge and improving the quality of epitaxial growth are helpful to improve the performance of the hetero-junction AlGaN-based p–i–n PDs.

Acknowledgements This work was supported by the National Natural Science Foundation of China (Grant Nos. 51472230, 61504144, 61574142, and 61322406), the Nation Key Research and Development Program of China (Grant No. 2016YFB0400900), The Jilin Provincial Science & Technology Department (Grant No. 20170520156JH and 20150519001JH). The CAS Interdisciplinary Innovation Team, the Youth Innovation Promotion Association of CAS (grant no. 2015171). The Independent Innovation Fund of the State Key Laboratory of Luminescence and Applications (Grant No. Y5523FM152) and the Open Fund of the State Key Laboratory of Luminescence and Applications (Grant No. SKLLA201301).

References

[1] P. Sandvik, K. Mi, F. Shahedipour, R. Mcclintock, A. Yasan, P. Kung, and M. Razeghi, J. Cryst. Growth **231**, 366 (2001).
[2] M. Razeghi, Proc. IEEE **90**, 1006 (2002).
[3] L. Sang, M. Liao, and M. Sumiya, Sensors **13**, 10482 (2013).
[4] M. A. Khan, M. Shatalov, H. P. Maruska, H. M. Wang, and E. Kuokstis, Jap. J. Appl. Phys. **44**, 7191 (2005).
[5] W. Yang, T. Nohova, S. Krishnankutty, R. Torreano, S. McPherson, and H. Marsh, Appl. Phys. Lett. **73**, 1086 (1998).
[6] U. Chowdhury, M. M. Wong, C. J. Collins, B. Yang, J. C. Denyszyn, J. C. Campbell, and R. D. Dupuis, J. Cryst. Growth **248**, 552 (2003).
[7] N. Biyikli, I. Kimukin, O. Aytur, and E. Ozbay, IEEE Photonic. Tech. Lett. **16**, 1718 (2004).

 © 2017 WILEY-VCH Verlag GmbH & Co. KGaA, Weinheim

[8] C. Collins, U. Chowdhury, M. Wong, B. Yang, A. Beck, R. Dupuis, and J. Campbell, Appl. Phys. Lett. **80**, 3754 (2002).
[9] R. McClintock, A. Yasan, K. Mayes, D. Shiell, S. Darvish, P. Kung, and M. Razeghi, Appl. Phys. Lett. **84**, 1248 (2004).
[10] E. Cicek, R. McClintock, C. Cho, B. Rahnema, and M. Razeghi, Appl. Phys. Lett. **103**, 191108 (2013).
[11] J. Racko, P. Benko, L. Harmatha, R. Granzner, M. Kittler, F. Schwierz, and J. Breza, Appl. Surf. Sci. **312**, 68 (2014).
[12] K. Köhler, S. Müller, R. Aidam, P. Waltereit, W. Pletschen, L. Kirste, H. P. Menner, W. Bronner, A. Leuther, R. Quay, M. Mikulla, O. Ambacher, R. Granzner, F. Schwierz, C. Buchheim, and R. Goldhahn, J. Appl. Phys. **107**, 053711 (2010).
[13] M. S. Miao, J. R. Weber, and C. G. Van de Walle, J. Appl. Phys. **107**, 123713 (2010).
[14] F. A. Marino, D. A. Cullen, D. J. Smith, M. R. McCartney, and M. Saraniti, J. Appl. Phys. **107**, 054516 (2010).
[15] J. Liu, Y. Zhou, J. Zhu, K. M. Lau, and K. J. Chen, IEEE Electron Dev. Lett. **27**, 10 (2006).
[16] L. Wang, W. Hu, X. Chen, and W. Lu, J. Appl. Phys. **108**, 054501 (2010).
[17] X. D. Wang, W. D. Hu, X. S. Chen, and W. Lu, IEEE Trans. Electron. Dev. **59**, 1393 (2012).
[18] Z. Shao, D. Chen, Y. Liu, H. Lu, R. Zhang, Y. Zheng, L. Li, and K. Dong, IEEE J. Sel. Top. Quant. **20**, 187 (2014).
[19] M. Hou, Z. Qin, C. He, L. Wei, F. Xu, X. Wang, and B. Shen, Electron. Mater. Lett. **11**, 1053 (2015).
[20] X. Wang, W. Hu, X. Chen, J. Xu, L. Wang, X. Li, and W. Lu, J. Phys. D: Appl. Phys. **44**, 405102 (2011).
[21] Y. Chen, H. Song, D. Li, X. Sun, H. Jiang, Z. Li, G. Miao, Z. Zhang, and Y. Zhou, Mater. Lett. **114**, 26 (2014).
[22] Z. G. Shao, D. J. Chen, H. Lu, R. Zhang, W. J. Luo, Y. D. Zheng, L. Li, and Z. H. Li, IEEE Electron. Device Lett. **35**, 372 (2014).
[23] A. Osinsky, S. Gangopadhyay, R. Gaska, B. Williams, M. A. Khan, D. V. Kuksenkov, and H. Temkin, Appl. Phys. Lett. **71**, 2334 (1997).
[24] D. Li, X. Sun, H. Song, Z. Li, Y. Chen, G. Miao, and H. Jiang, Appl. Phys. Lett. **98**, 011108 (2011).
[25] O. Ambacher, B. Foutz, J. Smart, J. Shealy, N. Weimann, K. Chu, M. Murphy, A. Sierakowski, W. Schaff, and L. Eastman, J. Appl. Phys. **87**, 334 (2000).
[26] E. Arslan, S. Ozcelik, and E. Ozbay, J. Appl. Phys. **105**, 023705 (2009).
[27] D. Yan, H. Lu, D. Cao, D. Chen, R. Zhang, and Y. Zheng, Appl. Phys. Lett. **97**, 153503 (2010).
[28] J. F. Muth, J. D. Brown, M. Johnson, Z. Yu, R. M. Kolbas, J. Cook and J. Schetzina, MRS Symp. Proc. **537**, G5. 2 (1998).
[29] S. C. Jain, M. Willander, J. Narayan, and R. V. Overstraeten, J. Appl. Phys. **87**, 965 (2000).

© 2017 WILEY-VCH Verlag GmbH & Co. KGaA, Weinheim